Modeling of Propeller Electric Airplane and Thrust Control using Advantage of Electric Motor

Kenichiro Takahashi, Hiroshi Fujimoto, and Yoichi Hori
Graduate School of Frontier Sciences,
The University of Tokyo
5-1-5 Kashiwanoha, Kashiwa-shi, Chiba, 277-8561 Japan
Phone and Fax: +81-4-7136-3881

Hiroshi Kobayashi and Akira Nishizawa
Institute of Aeronautical Technology
Japan Aerospace Exploration Agency
6-13-1 Osawa, Chofu-shi, Tokyo 181-0015
Telephone: +81-50-3362-4458

***Abstract*—Electrical airplanes (EAs) have become practical in the recent years. Considering the increase of demand on smaller aircraft and the attention to environmental issues, the demand on small EAs is expected to grow in the coming decade. However, the accident rate of small aircrafts is higher than that of larger aircrafts, so ensuring higher safety of EA is very urgent. In this paper, the new thrust control method based on new EA propeller plant is proposed. This method can be applied to new advanced flight control systems of EA, which can be expected to improve the safety of EA. The effectiveness of the proposed method is verified through simulations and experiments.**

I. Introduction

A. Background

Recently, light airplanes such as light general aviation is increasing rapidly [1]. However, business aircraft have a fatal accident rate approximately 10 times higher than that of large commercial jets [2], and improvement of safety is required. A great number of the accidents are caused by weather change, regardless of the size of the airplane [3], [4], and rising the safety verses weather is urgent.

Electric airplanes have become widely noticed for environmental reasons [5]. Furthermore, electric airplanes have not only environmental advantages, but electric motors have characteristics as listed below.

- The torque response of electric motors is 100-500 times faster than that of engines.
- The output torque can be measured accurately from the motor current.
- Dispersed placement and independent control can be done easily, and the flexibility of the plane design and the degree of freedom of control is higher.
- Physical energy can be regenerated to electric energy.

Many researches have been carried out with EVs using these merits [6], [7].

Technological exchange between the automotive and aviation industry have been active ever since the Wright brothers took flight [8]. If the airplane becomes motorized, the motion control theories highly developed in the automotive industry can be expected to be adapted to airplanes [9].

B. Objective

Including EAs, present airplanes are designed to give higher stability and controllability. For example, the wings of an airplane is swept back and has a dihedral angle, and the tail assemblies are designed large. However, these structures increase drag, or request higher strength which make the airplane heavier. One solution is to compensate the stability with control, but conventional airplanes only have three main control surfaces, and this is not enough to control the 6 degree of freedom the airplane has. The thrust is another factor that may be controlled, and thrust control method of engines have been researched [10], but the controlling of output torque is difficult, and the thrust control system is complex and the response speed is not high.

On the other hand, electric airplanes' thrust can be controlled easily due to the characteristics listed above. By developing high response accurate thrust control using electric motor, high performance airspeed control can be developed. Furthermore, by harmoniously controlling dispersed placed motor, completely new control methods that could not be adopted to conventional airplanes can be conceivable.

Therefore, this paper will propose a thrust control method as a basic study. The proposed method will be verified by simulation and experiment.

II. Modeling of Single Motor Electric Airplane

In this section, the single motor electric airplane will be modeled. First, the physics that determine thrust and counter torque will be explained. Than, the equation of motion is derived. Finally, the equations will be arranged into a block diagram as a model of the propeller airplane.

Fig. 1 is the cross section of a propeller blade at distance r from the hub. While flying, the propeller cross section moves as a composition of rotation and advance motion. Therefore, the cross section moves as a spiral. Assume the airspeed to be parallel with the axis of the propeller. Airspeed is the relative velocity between the air and airplane. When n is propeller revolution speed and $\boldsymbol{V}$ is the airspeed vector, the propeller cross section's airspeed $\boldsymbol{V}_r$ is the sum of revolution speed vector and airspeed vector as

$$\boldsymbol{V}_r = 2\pi r \boldsymbol{n} + \boldsymbol{V} \tag{1}$$

where $\boldsymbol{n}$ is a vector with a length of n with a rotation direction. Therefore, air stream attacks the propeller cross section as vector $-\boldsymbol{V}_r$.

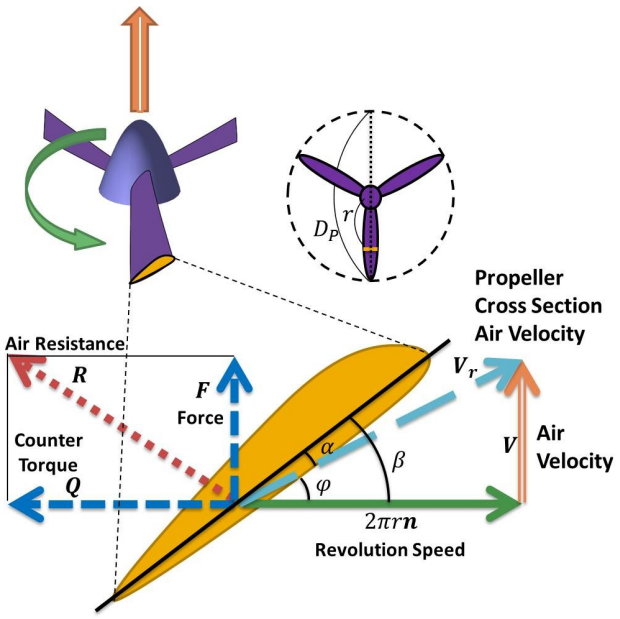

Fig. 1. Physics of propeller cross section [11]

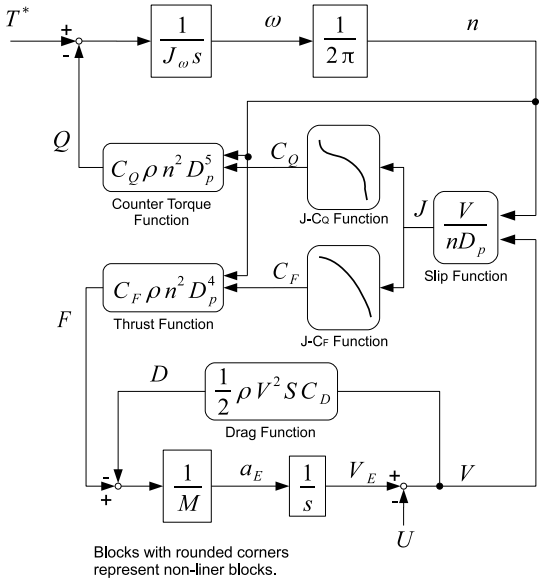

Fig. 2. Propeller model

The cross section takes a counter force vector $\boldsymbol{R}$. $\boldsymbol{R}$ can be resolved into the direction of the motion of the airplane vector $\boldsymbol{F}$, and the direction of propeller revolution vector $\boldsymbol{q}$.

$$\boldsymbol{R} = \boldsymbol{F} + \boldsymbol{Q}/r \tag{2}$$

The propeller cross section is a airfoil, so counter force $\boldsymbol{R}$ depend on the angle of attack α. Generally, it is known that the resolved force parallel to the air stream is increasing convex function of alpha, and the resolved force perpendicular to the air stream is a function with a peak.

The angle between vector $\boldsymbol{V}_r$ and the surface of propeller revolution φ is defined as angle of advance. The angle of attack α can be represented as

$$\alpha = \beta - \varphi \tag{3}$$

$$= \beta - \arctan\left\{\frac{1}{2\pi r} \cdot \frac{V}{n}\right\} \tag{4}$$

where β is the angle between the chord of blade of the propeller cross section and the revolution surface, $V = |\boldsymbol{V}|$, and $n = |\boldsymbol{n}|$. As shown in Eq. (4), the angle of attack α is a function of V/n. When advance ratio J is defined as a dimensionless equation as Eq. (5), $\boldsymbol{F}$ and $\boldsymbol{Q}$ is a function of J.

$$J = \frac{V}{nD_p} \tag{5}$$

From the above, when propeller counter torque $Q = |\boldsymbol{Q}|$ and thrust $F = |\boldsymbol{Q}|$ is represented as Eq. (6) and Eq. (7), dimensionless coefficient C_Q and C_F is a nonlinear function of J.

$$Q = C_Q \rho n^2 D_p^5 \tag{6}$$

$$F = C_F \rho n^2 D_p^4 \tag{7}$$

Here, ρ is air density.

A. Equation of Motion of Propeller and Body

Here, only the direction of movement is considered, and is assumed that airspeed and thrust change does not affect the attitude of the airplane. The propeller's equation of revolutionary motion and body's equation of translational motion is expressed as

$$J_\omega \dot{\omega} = T - Q, \qquad \omega = 2\pi n \tag{8}$$

$$M\dot{V}_E = F - D \tag{9}$$

where J_ω is the inertia moment of the propeller, ω is the angular velocity of the propeller, T is motor torque, M is plane mass, V_E is the relative speed between the ground and air, or ground speed, and D is drag.

By using drag coefficient C_D, drag D can be expressed as

$$C_D = \frac{D}{\frac{1}{2}\rho V^2 S} \tag{10}$$

where S is wing area.

The relation ship between airspeed V, groundspeed V_E, and tailwind U is expressed as

$$V = V_E - U. \tag{11}$$

From Eq. (8)–(11), the model of a single propeller airplane can be expressed as Fig. 2.

III. Designing of Thrust Control of Single Propeller Electric Airplane

In this section, new thrust control method with a inner loop of revolution speed control is proposed. Also in part III-D, the conventional method as a comparison of the proposed method is explained.

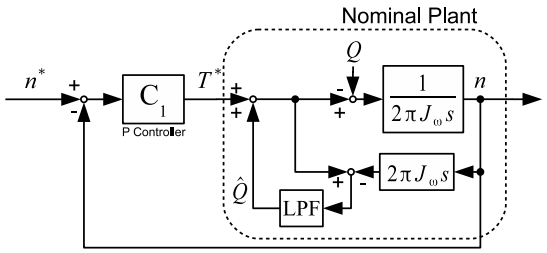

Fig. 3. Revolution speed controller

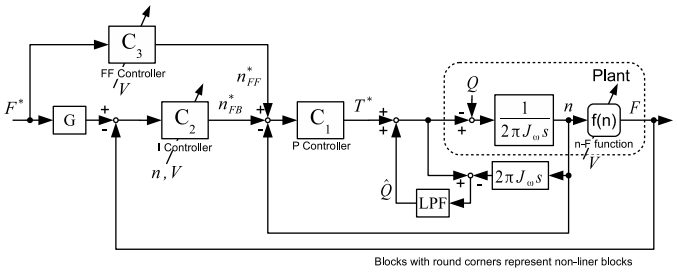

Fig. 4. Thrust controller

A. Designing of Propeller Counter Torque Observer

In this part, counter torque observer (CTO) is proposed. From Eq. (8), the propeller counter torque can be expressed as

$$Q = T - 2\pi J_\omega \dot{n}. \tag{12}$$

Therefore, if motor torque T and revolution speed n is detected, propeller counter torque $\hat{Q}$ can be estimated with a propeller counter torque observer as shown in Fig. 3. In this paper, it is assumed that the current controller is adequately fast to use motor torque command T^* for the estimation. By adding the estimated value to the torque command, the plant is nominalized as Eq. (13) at frequency ranges below the cutoff frequency ω_{C} of the low pass filter of the CTO.

$$n = \frac{1}{2\pi J_{\omega n} s} T \tag{13}$$

B. Designing of Revolution Speed Controller

In this part, the revolution speed controller is presented. The revolution speed controller is shown in Fig. 3. The revolution speed control is done by proportional controller. The gain C_1 of the proportional controller is decided so that the pole is placed at $-\omega_1$. Here, the plant is assumed to be the nominal plant $P_{1\mathrm{n}} := 1/2\pi J_{\omega n}$ as shown in Eq. (13).

The transfer function from n^* to n is express as Eq. (14), and is defined G_{nn^*}.

$$\frac{n}{n^*} = \frac{C_1 P_{1\mathrm{n}}}{s + C_1 P_{1\mathrm{n}}} = \frac{\omega_1}{s + \omega_1} = G_{nn^*} \tag{14}$$

C. Designing of Thrust Controller

In this part, the thrust controller is designed. The thrust controller is designed as a two-degree-of-freedom control as shown in Fig. 4.

C_F can be quadratically approximated. From Eq. (7), thrust F can be rewritten using coefficients a_{CF}, b_{CF}, and c_{CF} as

$$\begin{aligned} F &= \left(a_{\mathrm{CF}} J^2 + b_{\mathrm{CF}} J + c_{\mathrm{CF}}\right) \rho n^2 D_p^4 \\ &= c_{\mathrm{CF}} \rho D_p^4 n^2 + b_{\mathrm{CF}} \rho D_p^3 V n + a_{\mathrm{CF}} \rho D_p^2 V^2. \end{aligned} \tag{15}$$

Define function f as a function between revolution speed n and F as

$$F = f(n). \tag{16}$$

However, Thrust F is also a function of airspeed V, so V varies the non liner function f.

Feed forward controller C_3 is designed as follows. Thrust F is a function of n^* as

$$F = f(G_{nn^*} \cdot n^*). \tag{17}$$

Therefore,

$$\begin{aligned} n^* &= G_{nn^*}^{-1} \cdot f^{-1}(F) \\ &= \frac{s + \omega_1}{\omega_1} f^{-1}(F). \end{aligned} \tag{18}$$

Eq. (18) is non-proper, so feed forward controller C_2 is designed using reference model $G_0(s)$.

$$G_0(s) := \frac{\omega_g}{s + \omega_g} \tag{19}$$

$$n^* = f^{-1}(F) \cdot G_{nn^*}^{-1} \cdot G_0(s) \tag{20}$$

Here, ω_g is the pole of the reference model. Because $f^{-1}(F)$ varies by V and is non liner, feed forward controller C_2 is a non liner variable controller as shown in Eq. (20).

Next, feedback controller C_3 is designed as follows. Feedback reference F^*_{FB} is created by multiplying reference model $G_0(s)$ to thrust reference F^* as $F^*_{FB} = G_0(s)F^*$. By using Taylor series at operating point $n = n_0$, $f(n)$ can be approximated to its first order. When the first order coefficient is $a_F(n_0, V)$ and the intercept is $b_F(n_0, V)$, Eq. (21) is obtained.

$$F \approx a_F n + b_F \tag{21}$$

The revolution speed controller is assumed to be fast enough so $n = n^*$. The feed back controller uses the difference of the reference and output, so when b_F is regarded as a constant, Eq. (22) can be obtained as plant P_2.

$$P_2 := \frac{\Delta F}{\Delta n^*} = \frac{\Delta F}{\Delta n} = a_F \tag{22}$$

Thrust control uses integral controller, and the gain is decided so the pole is placed at $-\omega_2$ while the plant is assumed to be P_2. Here, a_F is a function of n_0 and V, so thrust feedback controller C_3 is a variable controller where n_0 is substituted by n successively.

D. Conventional Thrust Control Method of Propeller Engine Airplane

In this part, the conventional method as a comparison to the proposed method will be explained.

Conventional light airplanes with internal-combustion engine can only control propeller revolution speed. Accordingly, the conventional thrust control method is set up as follows.

TABLE I. PARAMETERS OF PROPELLER

Propeller Diameter D_p	178 mm
Propeller Inertia J_ω	1.06×10^{-5} kg·m
Air Density ρ	1.23 kg/m^3

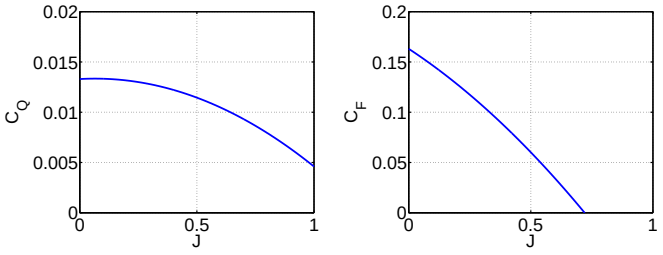

(a) $J - C_Q$ Curve (b) $J - C_F$ Curve

Fig. 5. Propeller characteristics

Assume that the pilot can give the revolution speed reference based on airspeed and thrust reference feed forwardly without any delay. The revolution speed control response speed is generally 2–3 seconds. This time needs to be ensured to keep safety according to the inertia moment of the reciprocal engine and the settling time of the fuel-air ratio.

In the simulations and experiments of this paper, revolution speed control will be presented as the identical controller as designed in part III-B, but the pole placed at ω_0 instead. The revolution speed reference is created by function f^{-1}.

IV. COMPARISON OF THRUST CONTROLLERS THROUGH SIMULATIONS

Thrust control method proposed in section III is verified by two simulations. The plants used for the simulations only consider the propeller's physics, and the body's dynamics were not considered. That is, the propeller was considered to operate at a given airspeed.

The poles of each controller were placed as following; the revolution speed controller at $\omega_0 = 0.4$ rad/s and $\omega_1 = 100$ rad/s, the pole of the thrust controller at $\omega_2 = 50$ rad/s, and the pole of the reference model at $\omega_g = 50$ rad/s.

The simulation model uses the parameter of APC 7x6 SF model propeller. The parameters are as listed in Table I. The J–C_Q curve and J–C_F curve is shown in Fig. 5(a) and Fig. 5(b) accordingly.

A. Step Response of Thrust

Step response simulation was carried out to the thrust controller. The airspeed was fixed, and a step reference was given. The airspeed V was set at $V = 7$ m/s, and the simulation started at a steady state of propeller revolution speed $n = 85.4$ rps and thrust $F = 0.60$ N. At $t = 1.0$, thrust reference changed from 0.60 N to 1.20 N.

The simulation result is shown in Fig. 6. Compared to the conventional method, the proposed method shows faster thrust response. Fast revolution speed response can be also seen. There is a small overshoot with the thrust control. It is conceivable that this happened because counter torque Q is also a result of n and V, and the CTO was not able to compensate the counter torque at high frequency.

B. Tailwind Disturbance Response

Next, the airspeed was changed mocking a tailwind gust with a fixed thrust reference.

The thrust reference was fixed at $F^* = 1.0$ N, and the simulation started at a steady state at propeller revolution speed of $n = 99.6$ rps and airspeed of $V = 7.00$ m/s. At $t = 0$, airspeed changed from 7.00 m/s to 6.00 m/s.

The simulation result is shown in Fig. 7. Both the conventional and proposed method's thrust rises when the airspeed changes. The conventional method changes the revolution speed reference according to the airspeed change. The revolution speed responds slowly, and the thrust recovers accordingly. On the other hand, the proposed method aggressively drops the revolution speed in order to recover thrust quickly.

V. COMPARISON OF THRUST CONTROLLERS THROUGH EXPERIMENT

The effectiveness of the proposed method was verified though two experiments.

A. Experimental Setup

In this part, the experimental unit made for this research will be explained. The experimental unit is shown in Fig. 8 and (9). The unit consists of liner guide, force sensor, motor mount, motor, encoder, propeller, anemometer, and wind tunnel.

The propeller is connected to the motor, and the thrust is measured by the force sensor. The propeller is set at 5 cm from the opening of the wind tunnel, so that the axis of the propeller is parallel with the wind. The anemometer is fixed at the opening of the wind tunnel. The size of the opening of the wind tunnel is 200 mm $\times$ 200 mm.

Because the anemometer is set in front of the propeller, even when the wind tunnel is set at same speed, the measured wind speed is enlarged. The speed of air in front of the propeller is also larger than the airspeed of a real airplane. This experimental unit does not have a wind tunnel large enough compared to the propeller, the airspeed was assumed that it is the measured value when the power given to the propeller was zero.

The pseudo-differentiation of the angle measured by the encoder was used acquire revolution speed. The controller's poles were placed equally with the simulation above. The parameters are shown in Table I.

B. Step Response of Thrust

Step response experiment was carried out to the thrust controller. The airspeed was fixed, and a step reference was given. The airspeed V was set at $V = 7$ m/s, and the simulation started at a steady state of thrust at $F = 0.60$ N. At $t = 1.0$, thrust reference changed from 0.60 N to 1.20 N.

The experiment results are shown in Fig. 10. In Fig. 10(a), the conventional method has a steady state error caused by modeling error that was not assumed in the simulation. On the

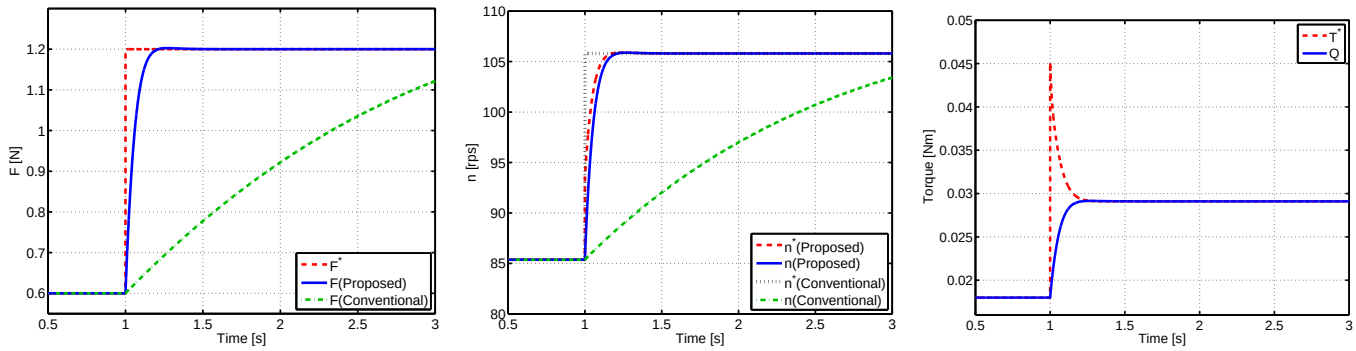

(a) Propeller thrust$F$ (b) Revolution speed n (c) Torque T^*, Counter torque Q

Fig. 6. Simulation results for step thrust command

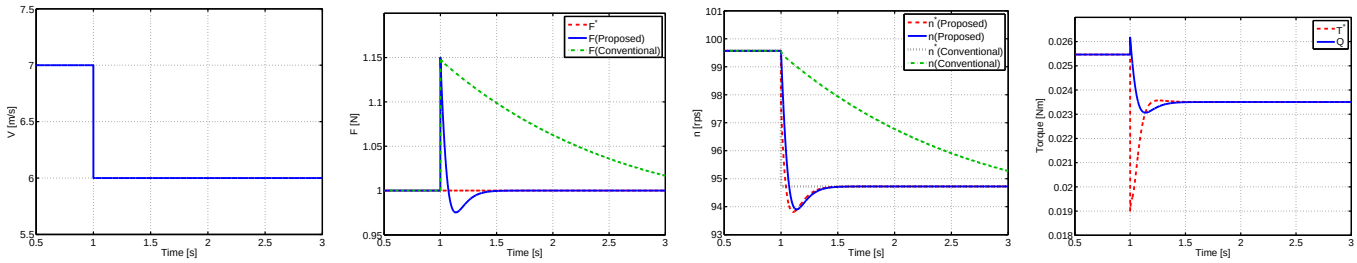

(a) Airspeed V (b) Thrust F (c) Revolution speed n (d) Torque T^*, Counter torque Q

Fig. 7. Simulation results for step airspeed change

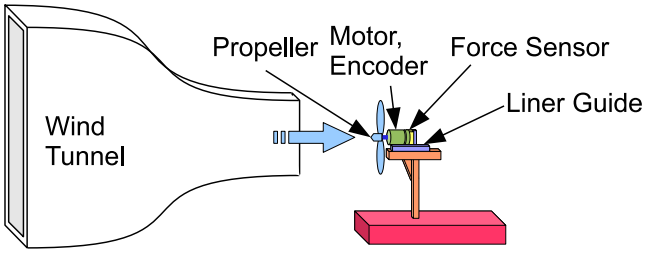

Fig. 8. Schematic Diagram of Experimental Unit

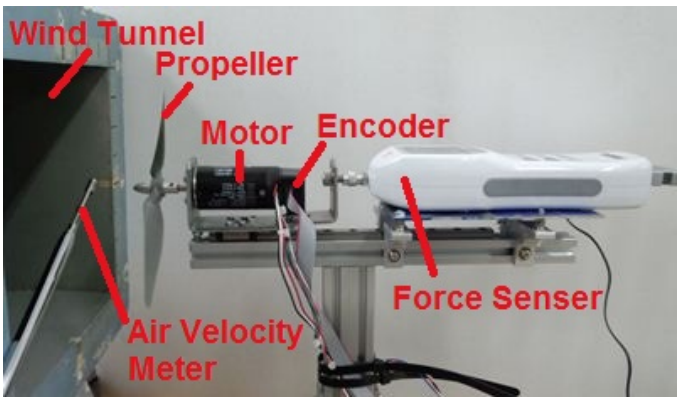

Fig. 9. Picture of Experimental Unit

other hand, the proposed method's thrust follows the reference quickly and accurately, despite of the small ripples.

These ripples can be assumed that they are the vibration that were transmitted from the propeller caused by axial deviation and wind turbulance. The revolution speed has small ripples cause by quantization and sampling errors of the encoder signals, and the counter torque calculated by using the revolution speed differential vibrates, causing the torque reference to also vibrate. It can be assumed that this is another cause of the thrust vibration.

C. Tailwind Disturbance Response

Next, the airspeed was changed mocking a tailwind gust with a fixed thrust reference.

The thrust reference was fixed at $F^* = 1.0$ N, and the experiment started at a steady state at airspeed of $V = 7.00$ m/s. At $t = 0$, the airspeed was changed by closing the intake of the wind tunnel. The airspeed eventually changed to $V = 0.36$ m/s.

In this experiment, the airspeed measured changes when the propeller is actively rotated, so the revolution speed controller was changed to unvariant controller.

The experiment results are shown in Fig. 10. Fig. 11(b) shows that the conventional method can not follow the reference when the airspeed changes. On the other hand, the proposed method's thrust only rises very shortly, and recovers the reference's thrust quickly. As soon as the difference between the real thrust and the reference thrust is detected, the revolution speed reference drops, making the torque reference to drop. This results to the drop of torque and revolution speed

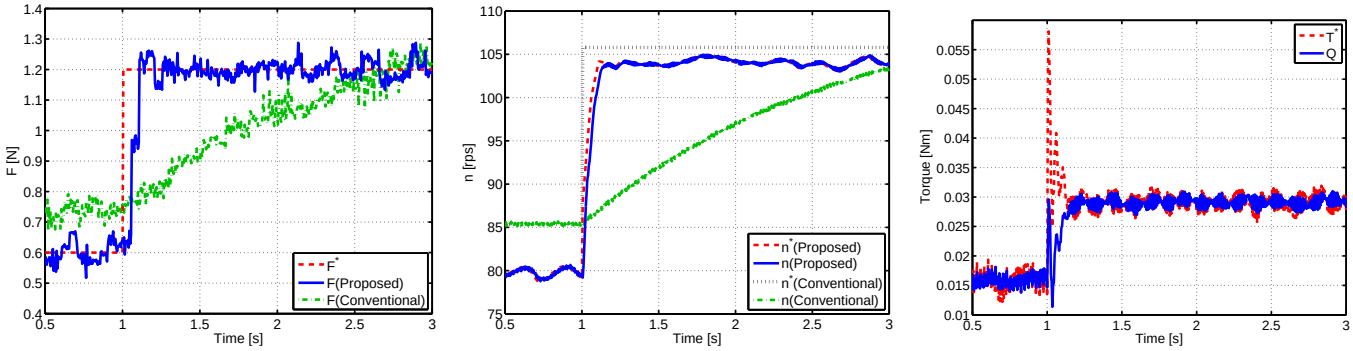

(a) Thrust F (b) Revolution Speed n (c) Torque T, Counter Torque $\hat{Q}$

Fig. 10. Experiment Results for Step Force Control

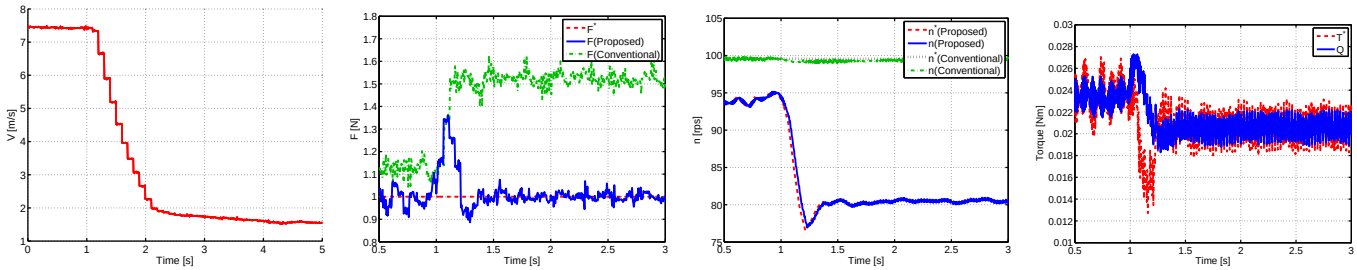

(a) Measured Airspeed (b) Thrust F (c) Revolution Speed n (d) Torque T, Counter Torque Q

Fig. 11. Experiment Results for Airspeed Change

making the thrust follow its reference.

VI. Conclusion

In this paper, a new thrust control method of a single propeller electric airplane for higher maneuverability was proposed. First, the single propeller electric airplane was modeled. Next, a thrust control method with a revolution speed control in the inner loop was proposed based on the proposed model. Finally, simulation and experiment was carried out, and the proposed method was verified to have quick and accurate response to the reference, and has high robustness to disturbance.

A airspeed control method was omitted from this paper due to limitations of space, but is published and read at 51th AIRCRAFT SYMPOSIUM hosted by JSASS [12].

References

[1] Michael P. Huerta: “FAA Aerospace Forecast Fiscal Years 2012-2032,” FAA Aerospace Forecast Fiscal Years 2012-2032, (2012).

[2] International Business Aviation Council: “Business aviation safety brief,” International Business Aviation Council, No. 10 (2011-9).

[3] Aviation Safety: “Statistical Summary of Commercial Jet Airplane Accidents,” Statistical summery, Boeing Commercial Airplanes (2011-6).

[4] R. Kebabjian: “Accident Statistics”. PlaneCrashInfo.com (2010).

[5] “The 2011 Green Flight Challenge Sponsored by Google,” CAFE Foundation. CAFE Foundation, Web. (2012).

[6] K. Nam, Y. Kim S. Oh, and Y. Hori: , ”Steering Angle-Disturbance Observer (SA-DOB) based yaw stability control for electric vehicles with in-wheel motors,” Control Automation and Systems (ICCAS), 2010 International Conference on , vol., no., pp.1303-1307 (2010-10).

[7] Y. Chen, J. Wang; ”Energy-efficient control allocation with applications on planar motion control of electric ground vehicles,” American Control Conference (ACC), 2011, pp.2719-2724 (2011-6).

[8] Venkatesh Prasad, K.; Broy, M.; Krueger, I., ”Scanning Advances in Aerospace & Automobile Software Technology,” Proceedings of the IEEE , vol.98, no.4, pp.510,514 (2010-4).

[9] A. Nishizawa, H. Kobayashi, K. Okai, and H. Fujimoto: “Progress of Electric Vehicle Technology and Future of Electric Aircraft,” The 43rd JSASS Annual Meeting, pp. 521–526 (2012) (in Japanese).

[10] T. Tucker: “Touchdown: The Development of Propulsion Controlled Aircraft at NASA Dryden,” Monographs in Aerospace History, No. 16, Washington (1999).

[11] Karl Falk: “Aircraft PRopeller Handbook,” The Ronald Press Company, New York (1937).

[12] Kenichiro Takahashi, Hiroshi Fujimoto, Yoichi Hori, Hiroshi Kobayashi, Akira Nishizawa, “Control of Electric Airplane’s Airspeed using Advantage of Electric Motor and Proposal of Test Method with Electric Vehicle”, 51th AIRCRAFT SYMPOSIUM (2013) (in Japanese).